

Proteomic analysis of isolated membrane fractions from superinvasive cancer cells

Paul Dowling^{*}, Paula Meleady, Andrew Dowd, Michael Henry, Sharon Glynn, Martin Clynes

National Institute for Cellular Biotechnology, Dublin City University, Glasnevin, Dublin 9, Ireland

Received 27 June 2006; received in revised form 4 August 2006; accepted 18 September 2006

Available online 30 September 2006

Abstract

The superinvasive phenotype exhibited by paclitaxel-selected variants of an *in vitro* invasive clonal population of the human cancer cell line, MDA-MB-435S were examined using DIGE (Fluorescence 2-D Difference Gel Electrophoresis) and mass spectrometry. Isolation of membrane proteins from the MDA-MB-435S-F/Taxol-10p4p and parental populations was performed by temperature-dependent phase partitioning using the detergent Triton X-114. Subsequent DIGE-generated data analysed using Decyder software showed many differentially-expressed proteins in the membrane fraction. 16 proteins showing statistically significant upregulation in the superinvasive cells were identified by MALDI-ToF. Proteins upregulated in the superinvasive population include Galectin-3, Cofilin, ATP synthase beta subunit, voltage-dependent anion channel 1, voltage dependent anion channel 2, ER-60 protein, MHC class II antigen DR52, Beta actin, TOMM40 protein, Enolase 1, Prohibitin, Guanine nucleotide-binding protein, Annexin II, Heat shock 70 kDa protein, Stomatin-like protein 2 and Chaperonin. Many of these proteins are associated with inhibition of apoptosis, the progression of cancer, tumourigenicity, metastasis, actin remodelling at the leading edge of cells, polarized cell growth, endocytosis, phagocytosis, cellular activation, cytokinesis, and pathogen intracellular motility. These results suggest a correlation between the increased abundance of these proteins with the superinvasive phenotype of the paclitaxel-selected MDA-MB-435S-F/Taxol-10p4p population.

© 2006 Elsevier B.V. All rights reserved.

Keywords: Cofilin; DIGE; Galectin-3; Membrane protein; Superinvasive

1. Introduction

The acquisition by cancer cells in the body of the metastatic phenotype (whereby cells invade into neighbouring tissues and across the blood or lymph vessel walls, travel in the blood or lymph to distant sites where they lodge, invade and proliferate) represents one of the most dangerous aspects of tumour progression [1]. No good *in vitro* models for metastasis exist, but recent research in our laboratory has identified an *in vitro* phenotype, which has been termed superinvasiveness [2] which appears to correlate with at least some aspects of the metastatic phenotype both *in vivo* and *in vitro* [3]. The molecular basis for the transition to the superinvasive phenotype is unknown. This paper focuses on the identification of relevant changes at the protein level in the membrane fraction of superinvasive cells as compared to their non-superinvasive parental cell lines.

The cells discussed in this paper display a novel phenotype, which we have termed ‘superinvasion’ in which cells not only digest their way through extracellular matrix and migrate through microtubules, as is standard in the Boyden Chamber assays, but also detach from the underside of the chamber, survive in suspension and re-attach to the surface of the microwell. This phenotype is indicative of aggressive metastasis-like behaviour.

Anticancer drugs, as well as killing some cells, can cause mutations in other cancer cells which survive. We have previously shown that drug exposure can result in the conversion of cells from a non-invasive to an invasive phenotype [2], and our identification of the superinvasive phenotype is a further observation of the multiple effects, not all desirable, which anticancer drugs can exert on cells.

We focused on the membrane fraction because invasion is a prerequisite for tumour metastasis and is associated with increased cellular motility, the production of enzymes with proteolytic activity and alterations in cell adhesion. Cell surface proteins play important roles in cell signalling, adaptation to

^{*} Corresponding author. Tel.: +353 1 7005700/8291; fax: +353 1 7005484.

E-mail address: paul.dowling@dcu.ie (P. Dowling).

environment and cell–matrix interactions, and so are likely to be involved in the acquisition and maintenance of invasive and metastatic properties of tumour cells. Identification of differentially expressed proteins between parental and superinvasive cells could therefore point to potential drug targets and diagnostic markers.

A CyDye™ DIGE fluorescent minimal labelling approach was used to enrich and detect cell surface proteins in MDA-MB-435S-F (parental clone) and MDA-MB-435S-F/Taxol-10p4p (superinvasive variant) cell lines [4]. Fractionated cell membrane proteins were separated using the fluorescent 2-D DIGE technology and protein spot maps were further analysed with DeCyder™ Differential Analysis Software.

2. Materials and methods

2.1. Chemicals

Paclitaxel was obtained from Bristol-Myers Squibb (Dublin, Ireland). All media and serum used in the maintenance of the cell lines were obtained from Sigma Aldrich (Dublin, Ireland). Immobilized 24 cm linear pH gradient (IPG) strips, pH 3–11, IPG Buffer and cyanine dyes Cy2, Cy3, and Cy5 were purchased from Amersham (Amersham Biosciences, Inc.) Protein Assay and membrane fractionation kits were purchased from Biorad (Biorad, Inc.). Unless stated, all other chemicals were obtained from Sigma (Dublin, Ireland).

2.2. Cell lines

The human breast cancer cell line MDA-MB-435S was obtained from the American type culture collection (ATCC) and was maintained in culture at 37 °C using RPMI 1640 supplemented with 2 mM L-glutamine (Gibco) and 10% foetal calf serum. MDA-MB-435S is a spindle-shaped strain which evolved from the parental line MDA-MB-435 isolated by Cailleau et al., 1978, derived from the pleural effusion of a 31-year-old female with metastatic, ductal adenocarcinoma of the breast [5]. In 2002, results were published suggesting that MDA-MB-435 was of melanoma origin [6]. It was recently reported that the MDA-MB-435 cells used widely have identical origins to those that exhibit a melanoma-like gene expression signature, but exhibit a small degree of genotypic and phenotypic drift [7], but the possibility that some breast tumours may have gene expression profiles similar to melanoma cannot be ruled out. MDA-MB-435S-F was obtained by clonal dilution from MDA-MB-435S in this laboratory. The MDA-MB-435S-F paclitaxel-resistant variants were derived by pulse selection of the parental cells with paclitaxel as previously described [2].

2.3. Invasion assays

Invasion assays were performed by a modification of the method previously described [8]. Matrigel was diluted to 1 mg/ml in serum-free DMEM medium. A volume of 100 µl of 1 mg/ml Matrigel was placed into each insert (Falcon) (8.0 µm pore size), which stood in wells of a 24-well plate (Costar). The inserts and the plate were incubated overnight at 4 °C. The following day, cells were harvested and suspended in RPMI 1640 containing 10% FCS at a concentration of 1×10^6 cells/ml. The inserts were washed with serum-free RPMI 1640, and then 100 µl of the cell suspension was added to each insert and 250 µl of RPMI 1640 containing 10% FCS was added to the insert well. Cells were incubated at 37 °C for 48 h. After this time period, the inner side of the insert was wiped with a wet swab to remove the cells, while the outer side of the insert was gently rinsed with PBS and stained with 0.25% crystal violet for 10 min, rinsed again and then allowed to dry. The surface of the 24-well plate was rinsed gently twice with PBS and stained with 0.25% crystal violet for 10 min, rinsed again and then allowed to dry. Cells were quantified by both counting with the aid of a light microscope and eluting the stain with 200 µl 33% glacial acetic acid. Aliquots (100 µl) were transferred to a 96-well plate and read in an ELISA reader at 570 nm with a reference wavelength of 620 nm.

2.4. Sample preparation and protein labelling

Cells at ~80% confluence were washed twice in phosphate-buffered saline, twice in sucrose buffer. Isolation of membrane proteins was performed on the subsequent cell pellet employing Triton X 114. This is based on the separation of membrane proteins by temperature-dependent phase partitioning using the detergent Triton X-114 [9,10]. After a final centrifugation step, the sample produces an upper aqueous phase and a lower detergent-rich phase. An insoluble pellet is also formed and is a source of more complex membrane proteins. Proteins extracted into the two phases are treated using the ReadyPrep 2-D cleanup kit (Biorad) to remove agents in the extraction process that interfere with IEF. The isolated membrane proteins were resuspended in buffer containing (4% (w/v) CHAPS, 7 M urea, 2 M Thiourea, 10 mM Tris–HCl, 5 mM Magnesium Acetate pH 8.5). Insoluble material was removed by centrifugation at 14,000 rpm for 20 min at 10 °C. Protein concentration was determined using the BSA protein assay kit (Biorad).

Cell lysates were labelled with N-hydroxy succinimidyl ester-derivatives of the cyanine dyes Cy2, Cy3, and Cy5 following the protocol described previously. Typically, 50 µg of lysate was minimally labelled with 200 pmol of either Cy3 or Cy5 for comparison on the same 2D gel. Labelling reactions were performed on ice in the dark for 30 min and then quenched with a 50-fold molar excess of free lysine to dye for 10 min on ice. A pool of all samples was also prepared and labelled with Cy2 to be used as a standard on all gels to aid image matching and cross-gel statistical analysis. The Cy3 and Cy5 labelling reactions (50 µg of each) from each lysate were mixed and run on the same gels with an equal amount (50 µg) of Cy2-labelled standard [4]. Replicates of 3 different biological samples were analysed in this experiment.

2.5. Protein separation by 2D gel electrophoresis and gel imaging

Immobilized 24 cm linear pH gradient (IPG) strips, pH 3–11, were rehydrated in rehydration buffer (7 M urea, 2 M Thiourea, 4% CHAPS, 0.5% IPG Buffer, 50 mM DTT) overnight, according to the manufacturer's guidelines. Isoelectric focusing was performed using an IPGphor apparatus (Amersham Biosciences, Inc.) for a total of 40 kV/h at 20 °C, 50 mA. Strips were equilibrated for 20 min in 50 mM Tris–HCl, pH 8.8, 6 M urea, 30% (v/v) glycerol, 1% (w/v) SDS containing 65 mM DTT and then for 20 min in the same buffer containing 240 mM iodoacetamide. Equilibrated IPG strips were transferred onto 18 × 20 cm 12.5% uniform polyacrylamide gels poured between low fluorescence glass plates. Strips were overlaid with 0.5% (w/v) low melting point agarose in running buffer containing bromophenol blue. Gels were run using the Ettan Dalt 6 apparatus (Amersham Biosciences, Inc.) at 2.5 W/gel for 30 min then 100 W in total at 10 °C until the dye front had run off the bottom of the gels. All the images were collected on a Typhoon 9400 Variable Mode Imager (Amersham Biosciences, Inc.). Statistics and quantitation of protein expression were carried out in Decyder software (Amersham Biosciences, Inc.).

2.6. Spot digestion and MALDI-ToF analysis

Excision of protein spots, trypsin digestion, and protein identification by mass spectrometric analysis using an Ettan MALDI-ToF Pro instrument from Amersham Biosciences was performed according to an established methodology. Preparative gels containing 300 µg of protein were fixed in 30% (v/v) methanol, 7.5% (v/v) acetic acid overnight and washed in water, and total protein was detected by post-staining with SyproRuby dye (Molecular Probes) for 3 h at room temperature or Colloidal Coomassie (Sigma) for 2 h at room temperature. Excess dye was removed by appropriate destaining/washing methods. SyproRuby stained gels were imaged using a Typhoon 9400 Variable Mode Imager (Amersham Biosciences, Inc.) at the appropriate excitation and emission wavelengths for the stain. The subsequent gel image was imported into the BVA module of DeCyder software and was matched to images generated from DIGE analysis. Spots of interest were selected and confirmed using this software for subsequent picking using an Ettan Spot Picker. Gel plugs were placed into a presiliconized 1.5 ml plastic tube for destaining, desalting and washing steps. The remaining liquid above the gel plugs was removed and sufficient acetonitrile was added in order to cover the gel plugs. Following shrinkage of the gel plugs, acetonitrile was removed and the protein-containing gel pieces were rehydrated for 5 min with a minimal volume of 100 mM

ammonium bicarbonate. An equal volume of acetonitrile was added and after 15 min of incubation the solution was removed from the gel plugs and the samples then dried down for 30 min using a vacuum centrifuge. Individual gel pieces were then rehydrated in digestion buffer (12.5 ng trypsin per μl of 10% Acetonitrile 40 mM Ammonium Bicarbonate) to cover the gel pieces. More digestion buffer was added if all the initial volume had been absorbed by the gel pieces. Exhaustive digestion was carried out overnight at 37 °C. After digestion, the samples were centrifuged at 12,000 $\times g$ for 10 min using a bench top centrifuge. The supernatant was carefully removed from each sample and placed into clean and silicized plastic tubes. Samples were stored at -70 °C until analysed by MS. For spectrometric analysis, mixtures of tryptic peptides from individual samples were desalted using Millipore C-18 Zip-Tips (Millipore) and eluted onto the sample plate with the matrix solution [5 mg/ml *a*-cyano-4-hydroxycinnamic acid in 50% acetonitrile/0.1% trifluoroacetic acid (v/v)]. Mass spectra were recorded using the MALDI ToF instrument operating in the positive reflector mode at the following parameters: accelerating voltage 20 kV; and pulsed extraction: on (focus mass 2500). Internal and external calibration was performed using trypsin autolysis peaks at m/z 842.50, m/z 2211.104 and Pep4 mix respectively. The mass spectra were analysed using MALDI evaluation software (Amersham Biosciences), and protein identification was achieved with the PMF Pro-Found search engine for peptide mass fingerprints.

2.7. Statistical analysis

Two-sided, Student's *t*-tests were used to analyze differences in protein levels between the parental line MDA-MB-435S-F and MDA-MB-435S-F/Taxol-10p4p membrane protein cell lysates. A *p*-value of less than 0.05 was considered statistically significant.

3. Results

3.1. Invasion assays

Fig. 1 describes the invasive capabilities of MDA-MB-435S-F. Fig. 1 shows that while MDA-MB-435S-F is highly invasive, selection with paclitaxel results in a more aggressive invasive phenotype characterised by a proportion of the invading cells detaching from the bottom of the insert and reattaching to the bottom of the 24-well plate (superinvasion), which was negligible in MDA-MB-435S-F. In vitro invasiveness for the positive control cell line RPMI-2650MI and negative control cell line RPMI-2650 [11] gave expected results (results not shown) and the super-invasive phenotype was not observed in the positive control, as previously reported. There is no apparent difference in morphology between MDA-MB-435S-F and MDA-MB-435S-F/Taxol-10p4p cells as shown in Fig. 2.

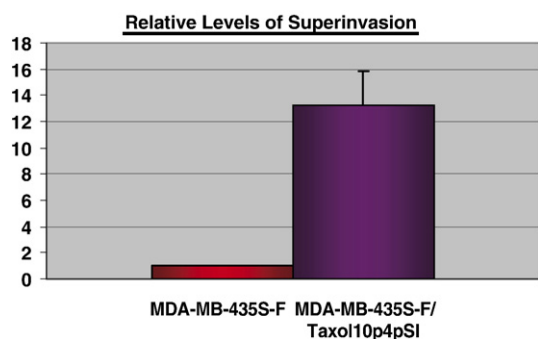


Fig. 1. Bar graph displaying the relative levels of superinvasion between MDA-MB-435S-F and MDA-MB-435S-F/Taxol10p4pSI phenotypes.

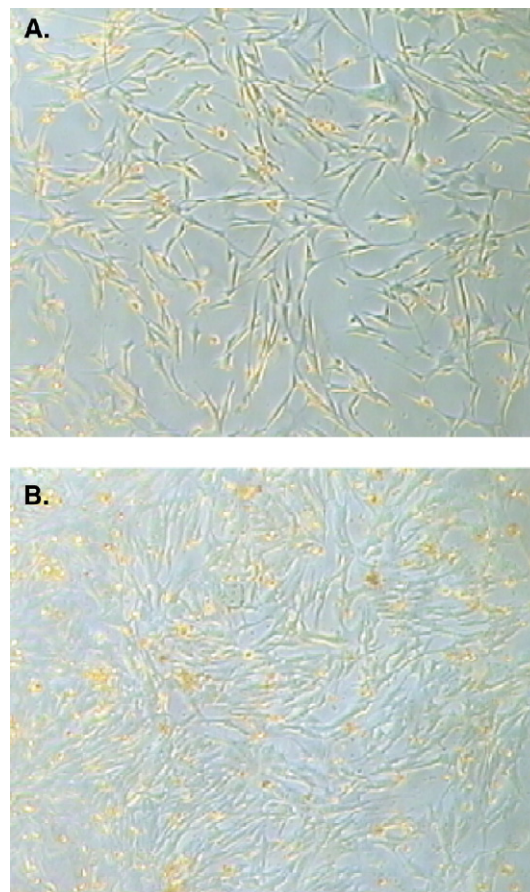


Fig. 2. Images showing the morphology of (A) MDA-MB-435S-F and (B) MDA-MB-435S-F/Taxol-10p4pSI cells.

3.2. DIGE analysis

Protein differences were analyzed using two-dimensional polyacrylamide gel electrophoresis (2D-PAGE, or 2D DIGE) to resolve proteins based on their isoelectric points and their molecular weight to generate a protein expression map (PEM) shown in Fig. 3. The PEMs of MDA-MB-435S-F and MDA-MB-435S-F/Taxol-10p4p can be compared and differentially expressed proteins of interest can be detected using an internal Cy2 labelled standard and DeCyder software. The precision of 2D DIGE is greatly improved if an internal standard is used with this biological technique as each sample can then be compared internally to the same standard, to account for any gel-to-gel variation.

Automatic spot detection using DeCyder software was followed by filtering of spots in each gel image to remove those that obviously originated from dust particles and gel impurities. After filtering, all six gels contained approximately 1500 protein spots. Automatic gel image matching was supplemented by manual addition of around 10 landmarks to guide the matching algorithm in subsequent re-matching attempts. Landmarks, which aid the matching process, were added in difficult areas, primarily near the edges/poor focusing and in areas with many spots. Proteins split into separate spots by the spot detection algorithm were manually merged during

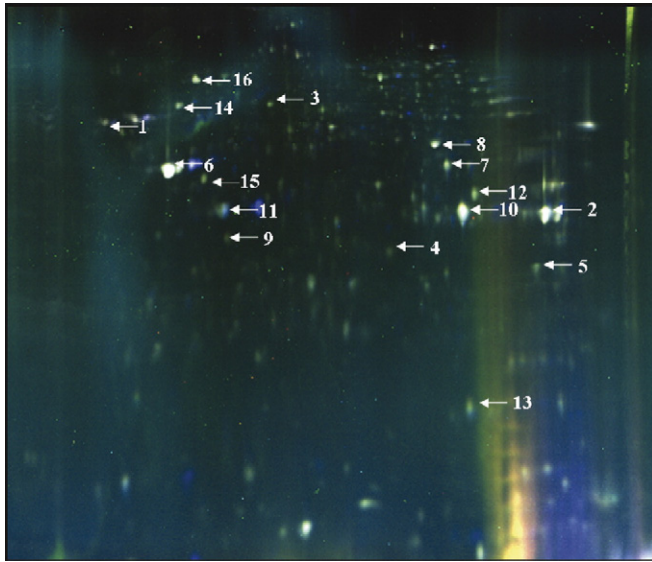


Fig. 3. 2D DIGE image of Cy 2, Cy 3 and Cy 5 labelled MDA-MB-435S-F and MDA-MB-435S-F/Taxol10p4pSI membrane proteins. Protein differences were analyzed using two-dimensional polyacrylamide gel electrophoresis (2D DIGE) to resolve proteins based on their isoelectric point, in this case a range of 3–11 was employed and their molecular weight to generate a protein expression map (PEM).

this process to improve matching. Proteins that were deemed to have statistically significant differential expression are listed in Table 1. Proteins listed in the table were overexpressed in the MDA-MB-435S-F/Taxol-10p4p phenotype compared with MDA-MB-435S-F, appeared in all six gels and attained a *t*-test score of less than 0.02. All proteins were digested and identified at least twice from separate gels with MALDI-ToF. An expectation value of zero denotes a perfect match; an expectation value of 0.01 indicates a 1% chance that the identification is random. All reported identifications have an expectation value of 0.01 or better. Other membrane proteins

were found to be up-regulated but they were expressed at such low levels that these proteins were not identified.

3.3. 3D images, statistics and mass spectrometry

Examples for the evaluation by DeCyder of alterations in spot intensities using the DIGE system are displayed in Fig. 4. To show visually alterations in corresponding spot intensity proportions, the selected spots for VDAC-1, Heat Shock 70 kDa protein, Galectin-3 and Cofilin are displayed as three-dimensional (3D) images. Fig. 4 also displays the associated graph views of standardized log abundances of the selected spots among analyzed gel replicates. VDAC-1 was 1.95-fold increased with a *t*-test score of 0.00012. Heat Shock 70 kDa protein was 1.77-fold increased with a *t*-test score of 8.10E-05. Galectin-3 was found to have an increased abundance of 1.71-fold in the superinvasive phenotype with a *t*-test score of 0.017 whereas Cofilin had an increased abundance of 1.81-fold with a *t*-test score of 0.0001.

A representative mass spectra for Heat Shock 70 kDa protein as displayed in Fig. 5 were recorded using the MALDI ToF instrument operating in the positive reflector mode at the following parameters: accelerating voltage 20 kV; and pulsed extraction: on (focus mass 2500). Internal and external calibration was performed using trypsin autolysis peaks at *m/z* 842.50, *m/z* 2211.104 and Pep4 mix respectively. The mass spectra were analysed using MALDI evaluation software (Amersham Biosciences), and protein identification was achieved with the PMF Pro-Found search engine for peptide mass fingerprints.

4. Discussion

A proteomics based approach was employed to look for changes in membrane protein expression contributing to the superinvasion seen in the MDA-MB-435S/Taxol-10p4p cell

Table 1
List of overexpressed proteins

Number	Name	<i>t</i> -test	Average ratio	Theoretical MW	Theoretical pI	%Coverage	Molecular function
1	ATP synthase beta subunit	0.00013	1.84	56.54	5.3	34.4	Transporter activity
2	Voltage-dependent anion channel 1	0.00012	1.95	30.74	8.8	55	Voltage-gated ion channel activity
3	ER-60 protein	0.00045	1.69	57.16	5.9	33.1	Isomerase activity
4	MHC class II antigen DR52	0.0033	1.56	27.22	6.8	34.6	MHC class II receptor activity
5	Galectin-3	0.017	1.71	26.19	8.6	11.2	Transcription regulator activity
6	Actin, beta	0.00059	1.85	40.83	5.8	32.8	Cytoskeletal protein
7	TOMM40 protein	0.0014	1.75	38.22	6.8	29.1	Transporter activity
8	ENO1 protein	5.80E-05	1.84	47.49	7	27.9	Catalytic activity
9	Prohibitin	0.0012	1.7	29.87	5.6	27.9	Receptor signaling complex scaffold activity
10	Voltage-dependent anion channel 2	0.00021	1.91	30.84	8.4	33.3	Voltage-gated ion channel activity
11	Guanine nucleotide-binding protein	0.0017	1.74	38.16	5.6	41.8	G protein
12	Annexin II isoform 2	6.70E-05	1.58	38.81	7.7	32.2	Calcium ion binding
13	Cofilin (non-muscle)	0.0001	1.81	18.71	8.5	32.5	Cytoskeletal associated protein
14	Heat shock 70 kDa	8.10E 05	1.77	53.61	5.6	33.1	Heat shock protein
15	Stomatin-like protein 2	0.00017	1.87	38.63	6.9	34.8	Unknown
16	Chaperonin	0.00014	1.82	61.21	5.7	23.4	Chaperone

Table of proteins found to be upregulated in MDA-MB-435S F/Taxol10p4pSI vs. MDA-MB-435S-F. Listed are the protein identities obtained from MALDI-ToF analysis, *t*-test score, average ratio, theoretical mw, theoretical pI, % coverage and molecular function.

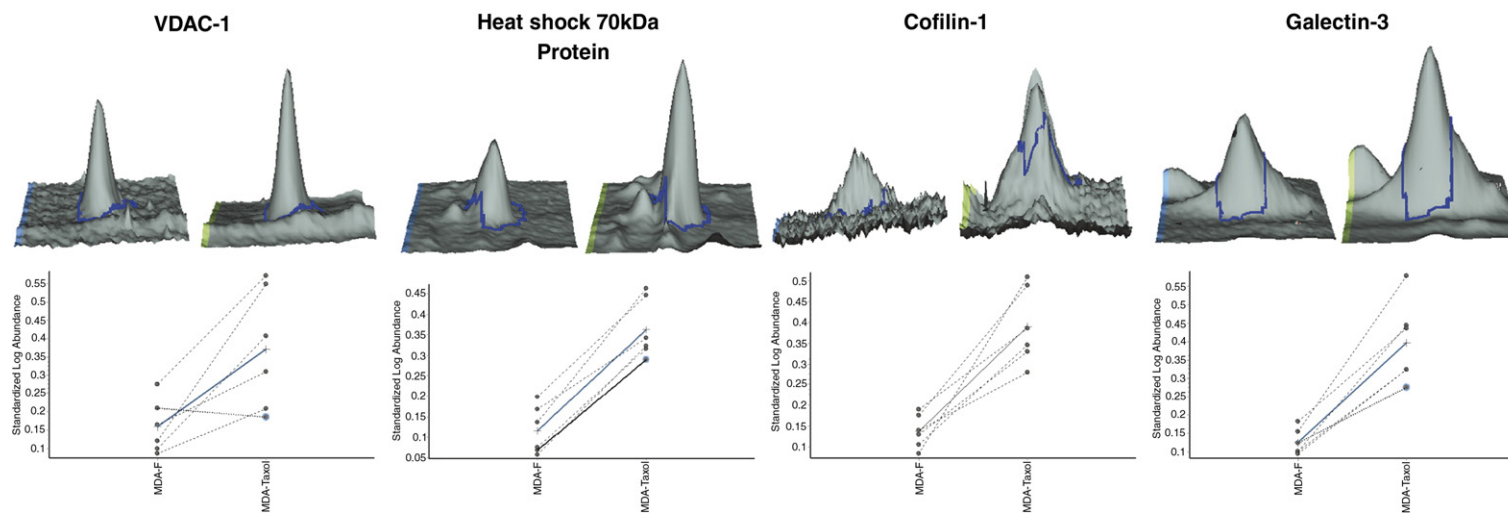


Fig. 4. 3-D images and Statistical analysis of voltage dependent anion channel 1, heat shock 70 kDa protein, cofilin-1 and galectin-3. Images and statistics were generated using the BVA module of DeCyder software.

population. DIGE analysis of isolated membrane fractions from MDA-MB-435S-F compared to MDA-MB-435S-F/Taxol-10p4p cell populations showed an increase in expression levels of many proteins.

Invasion and metastasis are complex processes involving many critical stages and Galectin-3 was found to be implicated in many of these including angiogenesis, cell matrix interactions and tumour embolism [12–14]. The superinvasive cells analysed in this study, display reduced attachment to ECM proteins coupled with increased motility [2]. Galectin-3 is involved in numerous cell–matrix and cell–cell interactions that could play a pivotal role in the invasive and metastatic potential of many cancers. Galectin-3 is known to function on the cell surface and in the extracellular environment [15], bind laminin, Lamp I and II, IgE and Mac-2 binding protein [16–18]. Carcinoma cells with high expression of galectin-3 such as MDA-MB-435 interact well and spread very rapidly on ECM proteins compared to those with low or no expression of galectin-3 such as BT-549 [19,20]. Downregulation of galectin-3 in MDA-MB-435 by the antisense approach has been reported to give rise to a subclone which spreads poorly, grows poorly in soft agar and forms tiny tumours in nude mice compared to the cells transfected with the empty vector [21].

Previous work on Galectin-3 in our laboratory showed that galectin-3 cDNA transfection into the human non-small cell lung carcinoma cell line, DLKP, resulted in enhanced adhesion to extracellular matrix components, cell motility and in vitro invasiveness. Furthermore, studies of RPMI-2650 variants suggest that galectin-3 expression correlates with nasal

carcinoma cell invasiveness [22]. Using the monoclonal antibody M3/38 that was raised against glycoprotein extracts, increased expression of Galectin-3 was observed in cancers from thyroid [23], central nervous system [24], head and neck squamous cell carcinoma [25], pancreas [26], bladder [27], stomach [28] and renal carcinoma [29].

High serum galectin-3 levels have been reported in advanced melanoma, with results suggesting that at least part of serum Gal-3 might be produced by metastatic melanoma tissue [30]. Galectin-3 and CD1a-positive dendritic cells are involved in the development of an invasive phenotype in vulvar squamous lesions and may provide novel additions for the diagnosis of invasion [31]. Galectin-3 enhances the metastatic potential of human breast carcinoma BT549 cells by increasing resistance to reactive nitrogen and oxygen species, such as NO and ONOO-, most likely through the bcl-2-like antiapoptotic function of galectin-3 [32]. The extracellular location of Galectin-3 on the cell surface and in the extracellular milieu indicates its participation in cell–cell and cell–matrix adhesion and interactions. These observations suggest potential for galectin-3 as a diagnostic/prognostic marker for specific cancer types and cancer stages.

Cofilin is an actin-modulating protein and our results point to an association with the superinvasive phenotype displayed by the MDA-MB-435S-F/Taxol-10p4p. Cofilin and beta actin were found to be overexpressed in the isolated membrane fraction from MDA-MB-435S-F/Taxol-10p4p cells.

Cell migration is a critical step in tumour invasion where reorganization of the actin cytoskeleton is the primary

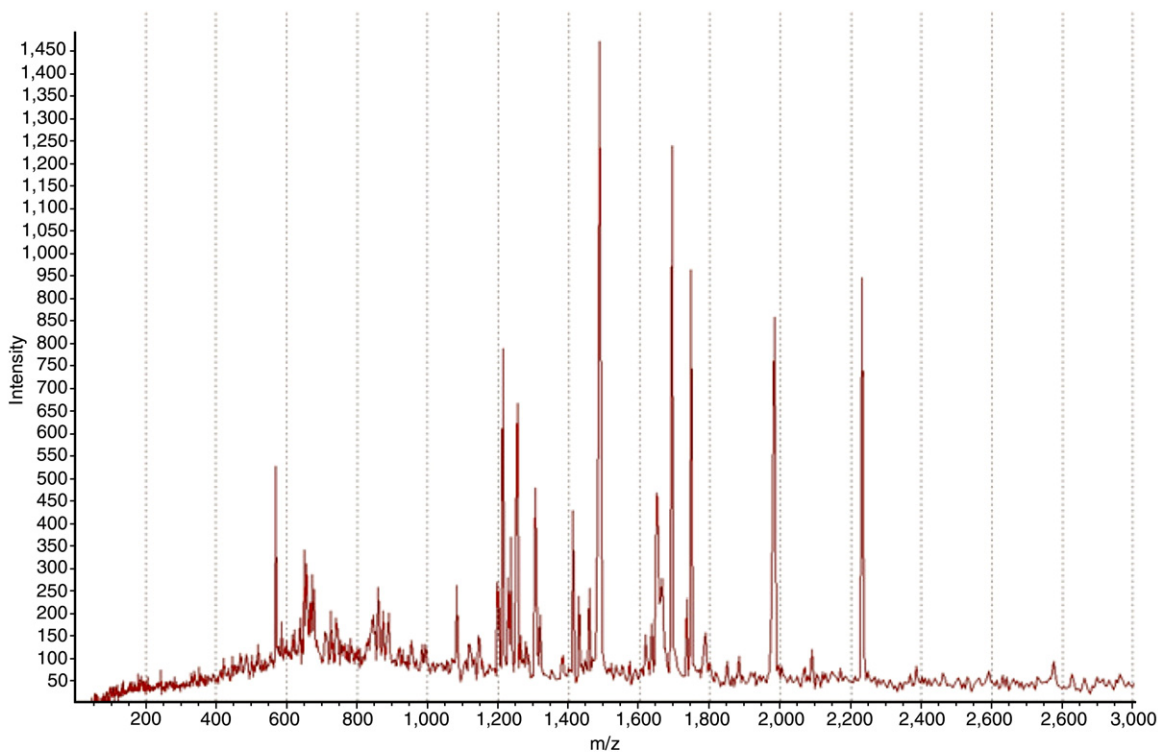


Fig. 5. Representative MALDI-ToF generated spectrum for heat shock 70 kDa protein. Protein identifications were achieved using the PMF Pro-Found search engine for peptide mass fingerprints.

mechanism of cell motility and is essential for most types of cell migration [33]. Cofilin has an important function as a critical regulator of actin dynamics and protrusive activity in cells [34], in particular the formation of invadopodia, which are membrane protrusions with a matrix degradation activity formed by invasive cancer cells [35]. However, molecular mechanisms that govern assembly and dynamics of invadopodia and the involvement of cofilin are still not well understood. An early step in cancer cell migration and invasion is the extension of cell protrusions in the direction of cell movement [1]. Cofilin nucleates actin polymerization by severing actin filaments to generate free barbed ends [36] and also increases the rate of actin depolymerization, thus maintaining a pool of actin monomer [37]. Cofilin is one of the essential components for *in vitro* reconstitution of *Listeria monocytogenes* motility that is driven by actin polymerization [38], and it has recently been reported that cofilin stimulates lamellipod protrusion and cell migration [39–41]. Yamaguchi et al. proposed a model for invadopodium formation where cofilin may be required for optimizing Arp2/3 complex-mediated dendritic nucleation to cause elongation of the invadopodia and its stabilization [34]. From our data the significant increase in the abundance of cofilin may have an important role in mechanisms associated with superinvasion.

Heat shock proteins (Hsps) are synthesized by cells in response to various stress conditions, including carcinogenesis, with Hsps found to be overexpressed in a wide collection of human cancers and are implicated in tumour cell proliferation, differentiation, invasion and metastasis [42–44]. Increased Hsp70 expression may also predict the response to some cancer treatments, for example in resistance to chemotherapy in breast cancer [45,46]. Our findings show that Hsp70 is overexpressed in MDA-MB-435S-F/Taxol10p4pSI cells compared to MDA-MB-435S-F cells and could be involved in the superinvasive phenotype and/or in the paclitaxel-resistance phenotype. Recently, differences in the expression of cell surface proteins between a normal prostate epithelial cell line (1542-NP2TX) and a prostate cancer cell line (1542-CP3TX) derived from the same patient were investigated, and results included the differential expression of VDAC-1 and VDAC-2 [47]. VDAC-1 and VDAC-2 were found to be 1.95-fold and 1.91-fold increased respectively in this study.

Other proteins found to be overexpressed were Annexin II, ENO1, SLP-2 and ATP synthase. Annexin II is a calcium- and phospholipid-binding protein and a substrate for protein-tyrosine kinases. Overexpression of Annexin II, which has been reported in various carcinomas, is thought to be associated with cell proliferation, differentiation, cell–cell adhesion and recently it was found that annexin II might be an important molecule in head and neck cancer invasion and metastasis. Annexin II heterotetramer (AII_t) has been shown to play an important role in degradation of extracellular matrix proteins, an important step for tumour cell local invasion, angiogenesis, and metastasis [48–50].

ENO1 is involved in the glycolytic pathway and was found to be significantly overexpressed in the HER-2/*neu*-positive breast tumours. HER-2/*neu* is overexpressed in up to 30% of breast cancers and is associated with poor prognosis and an

increased likelihood of metastasis especially in node-positive tumours. Takashima et al. showed that expression of alpha enolase also correlated positively with tumour size and venous invasion in hepatitis C virus-related hepatocellular carcinoma (HCV-related HCC). These results suggest that alpha enolase is a candidate biomarker for tumour progression [51,52]. SLP-2 is a novel and unusual member of the stomatin gene superfamily. Zhang et al. showed that SLP-2 was overexpressed in all tumour types they tested compared with their normal counterparts. Decreased cell growth, cell adhesion, and tumourigenesis in the antisense transfectants revealed that SLP-2 may be important in tumourigenesis [53–56].

ATP synthase occurs on the extracellular surface of a variety of cancer cells and Choi et al. showed that treatment with *N*-(4-methyl)phenyl-*O*-(4-methoxy)phenyl-thionocarbamate (MMTC) suppressed the metastasis of SK-MEL-8 cells and is associated with reduced levels of ATP synthase. Angiostatin, an antitumourigenic and antiangiogenic agent has been found to act through a mechanism implicating tumour cell surface ATP synthase [57,58].

In summary, selection of MDA-MB-435S-F with paclitaxel generated a superinvasive population of cells, namely MDA-MB-435S-F/Taxol-10p4p that is associated with upregulation of many proteins isolated from membrane fractions. All proteins listed have been implicated in tumour cell proliferation, differentiation, invasion and metastasis to a greater or lesser extent. It is probable that no single protein is responsible for the superinvasive phenotype investigated in this study and it is likely, based on the data presented here, that numerous proteins are involved.

Acknowledgement

This work was supported by the PRTL Cycle 3, programme of the Irish Higher Education Authority.

References

- [1] P. Friedl, K. Wolf, Tumour-cell invasion and migration: diversity and escape mechanisms, *Nat. Rev., Cancer* 3 (2003) 362–374.
- [2] S.A. Glynn, P. Gammell, M. Heenan, R. O'Connor, Y. Liang, J. Keenan, M. Clynes, A new superinvasive *in vitro* phenotype induced by selection of human breast carcinoma cells with the chemotherapeutic drugs paclitaxel and doxorubicin, *Br. J. Cancer* 91 (2004) 1800–1807.
- [3] S.A. Glynn, A. Adams, B. Gibson, D. Cronin, J.H. Harmey, M. Clynes, Low adhesiveness coupled with high superinvasiveness *in vitro* predicts the *in vivo* metastatic potential of a mouse mammary adenocarcinoma cell line, *Anticancer Res.* 26 (2006) 1001–1010.
- [4] A. Alban, S.O. David, L. Bjorkesten, C. Andersson, E. Sloge, S. Lewis, I. Currie, A novel experimental design for comparative two-dimensional gel analysis: two-dimensional difference gel electrophoresis incorporating a pooled internal standard, *Proteomics* 3 (2003) 36–44.
- [5] R. Cailleau, M. Olive, Q.V. Cruciger, Long-term human breast carcinoma cell lines of metastatic origin: preliminary characterization, *In Vitro* 14 (1978) 911–915.
- [6] G. Ellison, T. Klinowska, R.F. Westwood, E. Docter, T. French, J.C. Fox, Further evidence to support the melanocytic origin of MDA-MB-435, *Mol. Pathol.* 55 (2002) 294–299.
- [7] J.M. Rae, S.J. Ramus, M. Waltham, J.E. Armes, I.G. Campbell, R. Clarke, R.J. Barndt, M.D. Johnson, E.W. Thompson, Common origins of MDA-

- MB-435 cells from various sources with those shown to have melanoma properties, *Clin. Exp. Metastasis* 21 (2004) 543–552.
- [8] A. Albini, A. Melchiori, L. Santi, L.A. Liotta, P.D. Brown, W.G. Stetler-Stevenson, Tumor cell invasion inhibited by TIMP-2, *J. Natl. Cancer Inst.* 83 (1991) 775–779.
- [9] C. Bordier, Phase separation of integral membrane proteins in Triton X-114 solution, *J. Biol. Chem.* 256 (1981) 1604–1607.
- [10] V. Santoni, S. Kieffer, D. Desclaux, F. Masson, T. Rabilloud, Membrane proteomics: use of additive main effects with multiplicative interaction model to classify plasma membrane proteins according to their solubility and electrophoretic properties, *Electrophoresis* 21 (2000) 3329–3344.
- [11] Y. Liang, P. Meleady, I. Cleary, S. McDonnell, L. Connolly, M. Clynes, Selection with melphalan or paclitaxel (Taxol) yields variants with different patterns of multidrug resistance, integrin expression and in vitro invasiveness, *Eur. J. Cancer* 37 (2001) 1041–1052.
- [12] P. Nangia-Makker, Y. Honjo, R. Sarvis, S. Akahani, V. Hogan, K.J. Pienta, A. Raz, Galectin-3 induces endothelial cell morphogenesis and angiogenesis, *Am. J. Pathol.* 156 (2000) 899–909.
- [13] P. Warfield, Regulation of cellular adhesion to extracellular matrix proteins by galectin-3, *Biochem. Biophys. Res. Commun.* 246 (1998) 788–791.
- [14] H. Inohara, S. Akahani, K. Kohs, A. Raz, Interactions between galectin-3 and Mac-2-binding protein mediate cell–cell adhesion, *Cancer Res.* 56 (1996) 4530–4534.
- [15] B.J. Cherayil, S.J. Weiner, S. Pillai, The Mac-2 antigen is a galactose-specific lectin that binds IgE, *J. Exp. Med.* 170 (1989) 1959–1972.
- [16] H. Inohara, A. Raz, Identification of human melanoma cellular and secreted ligands for galectin-3, *Biochem. Biophys. Res. Commun.* 201 (1994) 1366–1375.
- [17] I. Rosenberg, B.J. Cherayil, K.J. Isselbacher, S. Pillai, Mac-2-binding glycoproteins. Putative ligands for a cytosolic beta-galactoside lectin, *J. Biol. Chem.* 266 (1991) 18731–18736.
- [18] H.J. Woo, L.M. Shaw, J.M. Messier, A.M. Mercurio, The major nonintegrin laminin binding protein of macrophages is identical to carbohydrate binding protein 35 (Mac-2), *J. Biol. Chem.* 265 (1990) 7097–7099.
- [19] P.R. Warfield, P.N. Makker, A. Raz, J. Ochieng, Adhesion of human breast carcinoma to extracellular matrix proteins is modulated by galectin-3, *Invasion Metastasis* 17 (1997) 101–112.
- [20] P. Matarrese, O. Fusco, N. Tinari, C. Natoli, F.T. Liu, M.L. Semeraro, W. Malorni, S. Iacobelli, Galectin-3 overexpression protects from apoptosis by improving cell adhesion properties, *Int. J. Cancer* 85 (2000) 545–554.
- [21] Y. Honjo, P. Nangia-Makker, H. Inohara, A. Raz, Down-regulation of galectin-3 suppresses tumorigenicity of human breast carcinoma cells, *Clin. Cancer Res.* 7 (2001) 661–668.
- [22] L. O'Driscoll, R. Linehan, Y.H. Liang, H. Joyce, I. Oglesby, M. Clynes, Galectin-3 expression alters adhesion, motility and invasion in a lung cell line (DLKP), *in vitro*, *Anticancer Res.* 22 (2002) 3117–3125.
- [23] D. Cvejic, S. Savin, I. Paunovic, S. Tatic, M. Havelka, J. Sinadinovic, Immunohistochemical localization of galectin-3 in malignant and benign human thyroid tissue, *Anticancer Res.* 18 (1998) 2637–2642.
- [24] R.S. Bresalier, P.-S. Yan, J.C. Byrd, R. Lotan, A. Raz, Expression of the endogenous galactose-binding protein galectin-3 correlates with the malignant potential of tumors in the central nervous system, *Cancer* 80 (1997) 776–787.
- [25] A. Gillenwater, X.C. Xu, A.K. el-Naggar, G.L. Clayman, R. Lotan, Expression of galectins in head and neck squamous cell carcinoma, *Head Neck* 18 (1996) 422–432.
- [26] C. Schaffert, P.M. Pour, W.G. Chaney, Localization of galectin-3 in normal and diseased pancreatic tissue, *Int. J. Pancreatol.* 23 (1998) 1–9.
- [27] L. Cindolo, G. Benvenuto, P. Salvatore, R. Pero, G. Salvatore, V. Mirone, D. Prezioso, V. Altieri, C.B. Bruni, L. Chiariotti, Galectin-1 and galectin-3 expression in human bladder transitional-cell carcinomas, *Int. J. Cancer* 84 (1999) 39–43.
- [28] S.E. Baldus, T.K. Zirbes, M. Weingarten, S. Fromm, J. Glossmann, F.G. Hanisch, S.P. Monig, W. Schroder, U. Flucke, J. Thiele, A.H. Holscher, H.P. Dienes, Increased galectin-3 expression in gastric cancer: correlations with histopathological subtypes, galactosylated antigens and tumor cell proliferation, *Tumour Biol.* 21 (2000) 258–266.
- [29] A.N. Young, M.B. Amin, C.S. Moreno, S.D. Lim, C. Cohen, J.A. Petros, F.F. Marshall, A.S. Neish, Expression profiling of renal epithelial neoplasms: a method for tumor classification and discovery of diagnostic molecular markers, *Am. J. Pathol.* 158 (2001) 1639–1651.
- [30] P. Vereecken, K. Zouaoui-Boudjeltia, C. Debray, A. Awada, I. Legssyer, F. Sales, M. Petein, M. Vanhaeverbeek, G. Ghanem, M. Heenen, High serum galectin-3 in advanced melanoma: preliminary results, *Clin. Exp. Dermatol.* 31 (2006) 105–109.
- [31] H. Brustmann, Galectin-3 and CD11a-positive dendritic cells are involved in the development of an invasive phenotype in vulvar squamous lesions, *Int. J. Gynecol. Pathol.* 25 (2006) 30–37.
- [32] Y.K. Song, T.R. Billiar, Y.J. Lee, Role of galectin-3 in breast cancer metastasis. Involvement of nitric oxide, *Am. J. Pathol.* 160 (2002) 1069–1075.
- [33] D. Yamazaki, S. Kurisu, T. Takenawa, Regulation of cancer cell motility through actin reorganization, *Cancer Sci.* 96 (2005) 379–386.
- [34] H. Yamaguchi, M. Lorenz, S. Kempiak, C. Sarmiento, S. Coniglio, M. Symons, J. Segall, R. Eddy, H. Miki, T. Takenawa, J. Condeelis, Molecular mechanisms of invadopodium formation: the role of the N-WASP-Arp2/3 complex pathway and cofilin, *J. Cell Biol.* 168 (2005) 441–452.
- [35] W.T. Chen, Proteolytic activity of specialized surface protrusions formed at rosette contact sites of transformed cells, *J. Exp. Zool.* 251 (1989) 167–185.
- [36] J. Condeelis, How is actin polymerization nucleated in vivo? *Trends Cell Biol.* 11 (2001) 288–293.
- [37] M.F. Carlier, F. Ressad, D. Pantaloni, Control of actin dynamics in cell motility. Role of ADF/cofilin, *J. Biol. Chem.* 274 (1999) 33827–33830.
- [38] T.P. Loisel, R. Boujemaa, D. Pantaloni, M.F. Carlier, Reconstitution of actin-based motility of *Listeria* and *Shigella* using pure proteins, *Nature* 401 (1999) 613–616.
- [39] A.Y. Chan, M. Bailly, N. Zebda, J.E. Segall, J.S. Condeelis, Role of cofilin in epidermal growth factor-stimulated actin polymerization and lamellipod protrusion, *J. Cell Biol.* 148 (2000) 531–542.
- [40] H.R. Dawe, L.S. Minamide, J.R. Bamburg, L.P. Cramer, ADF/cofilin controls cell polarity during fibroblast migration, *Curr. Biol.* 13 (2003) 252–257.
- [41] M. Ghosh, X. Song, G. Mouneimne, M. Sidani, D.S. Lawrence, J.S. Condeelis, Cofilin promotes actin polymerization and defines the direction of cell motility, *Science* 304 (2004) 743–746.
- [42] D. Atkins, R. Lichtenfels, B. Seliger, Heat shock proteins in renal cell carcinomas, *Contrib. Nephrol.* 148 (2005) 35–56.
- [43] X. Thomas, L. Campos, C. Mounier, J. Cornillon, P. Flandrin, Q.H. Le, S. Piselli, D. Guyotat, Expression of heat-shock proteins is associated with major adverse prognostic factors in acute myeloid leukemia, *Leuk. Res.* 29 (2005) 1049–1058.
- [44] T.S. Hwang, H.S. Han, H.K. Choi, Y.J. Lee, Y.J. Kim, M.Y. Han, Y.M. Park, Differential, stage-dependent expression of Hsp70, Hsp110 and Bcl-2 in colorectal cancer, *J. Gastroenterol. Hepatol.* 18 (2003) 690–700.
- [45] L.M. Vargas-Roig, F.E. Gago, O. Tello, J.C. Aznar, D.R. Ciocca, Heat shock protein expression and drug resistance in breast cancer patients treated with induction chemotherapy, *Int. J. Cancer* 79 (1998) 468–475.
- [46] D.R. Ciocca, V.R. Rozados, F.D. Cuello-Carrion, S.I. Gervasoni, P. Matar, O.G. Scharovsky, Hsp25 and Hsp70 in rodent tumors treated with doxorubicin and lovastatin, *Cell Stress Chaperones* 8 (2003) 26–36.
- [47] C. Hastie, M. Saxton, A. Akpan, R. Cramer, J.R. Masters, S. Naaby-Hansen, Combined affinity labelling and mass spectrometry analysis of differential cell surface protein expression in normal and prostate cancer cells, *Oncogene* 24 (2005) 5905–5913.
- [48] J. Mai, D.M. Waisman, B.F. Sloane, Cell surface complex of cathepsin B/annexin II tetramer in malignant progression, *Biochim. Biophys. Acta* 1477 (2000) 215–230.
- [49] K.A. Hajjar, S.S. Acharya, Annexin II and regulation of cell surface fibrinolysis, *Ann. N. Y. Acad. Sci.* 902 (2000) 265–271.
- [50] D.A. Siever, H.P. Erickson, Extracellular annexin, *Int. J. Biochem. Cell Biol.* 29 (1997) 1219–1223.
- [51] D. Zhang, L.K. Tai, L.L. Wong, L.-L. Chiu, S.K. Sethi, E.S.C. Koay, Proteomic study reveals that proteins involved in metabolic and

- detoxification pathways are highly expressed in HER-2/neu-positive breast cancer, *Mol Cell Proteomics* 4 (2005) 1686–1696.
- [52] M. Takashima, Y. Kuramitsu, Y. Yokoyama, N. Iizuka, M. Fujimoto, T. Nishisaka, K. Okita, M. Oka, K. Nakamura, Overexpression of alpha enolase in hepatitis C virus-related hepatocellular carcinoma: association with tumor progression as determined by proteomic analysis, *Proteomics* 5 (2005) 1686–1692.
- [53] Y. Wang, J.S. Morrow, Identification and characterization of human SLP-2, a novel homologue of stomatin (Band 7.2b) present in erythrocytes and other tissues, *J. Biol. Chem.* 275 (2000) 8062–8071.
- [54] G. Seidel, R. Prohaska, Molecular cloning of hSLP-1, a novel human brain-specific member of the band 7/MEC-2 family similar to *Caenorhabditis elegans* UNC-24, *Gene* 225 (1998) 23–29.
- [55] R.R. Sprenger, D. Speijer, J.W. Back, C.G. De Koster, H. Pannekoek, A.J. Horrevoets, Comparative proteomics of human endothelial cell caveolae and rafts using two-dimensional gel electrophoresis and mass spectrometry, *Electrophoresis* 25 (2004) 156–172.
- [56] L. Zhang, F. Ding, W. Cao, Z. Liu, W. Liu, Z. Yu, Y. Wu, W. Li, Y. Li, Z. Liu, Stomatin-like protein 2 is overexpressed in cancer and involved in regulating cell growth and cell adhesion in human esophageal squamous cell carcinoma, *Clin Cancer Res.* 12 (2006) 1639–1646.
- [57] S.L. Choi, Y.S. Choi, Y.K. Kim, N.D. Sung, C.W. Kho, B.C. Park, E.M. Kim, J.H. Lee, K.M. Kim, M.Y. Kim, P.K. Myung, Proteomic analysis and the antimetastatic effect of *N*-(4-methyl) phenyl-*O*-(4-methoxy) phenyl-thionocarbamate-induced apoptosis in human melanoma SK-MEL-28 cells, *Arch. Pharm. Res.* 29 (2006) 224–234.
- [58] S.L. Chi, S.V. Pizzo, Angiostatin is directly cytotoxic to tumor cells at low extracellular pH: a mechanism dependent on cell surface-associated ATP synthase, *Cancer Res.* 66 (2006) 875–882.